Published in final edited form as:
Eur Biophys J. 2009 September ; 38(7): 847–855. doi:10.1007/s00249-009-0444-y.

The binding of analogs of porphyrins and chlorins with elongated side chains to albumin

Shimshon Ben Dror,
Department of Physics, Nano Medicine Research Center, Institute of Nanotechnology and Advanced Materials, Bar Ilan University, 52900 Ramat Gan, Israel

Irena Bronshtein,
Department of Physics, Nano Medicine Research Center, Institute of Nanotechnology and Advanced Materials, Bar Ilan University, 52900 Ramat Gan, Israel

Hana Weitman,
Department of Physics, Nano Medicine Research Center, Institute of Nanotechnology and Advanced Materials, Bar Ilan University, 52900 Ramat Gan, Israel

Kevin M. Smith,
Department of Chemistry, Louisiana State University, Baton Rouge, LA 70803, USA

William G. O'Neal,
Department of Chemistry, Dartmouth College, Hanover, NH 03755, USA

Peter A. Jacobi, and
Department of Chemistry, Dartmouth College, Hanover, NH 03755, USA

Benjamin Ehrenberg
Department of Physics, Nano Medicine Research Center, Institute of Nanotechnology and Advanced Materials, Bar Ilan University, 52900 Ramat Gan, Israel

Abstract

In previous studies, we demonstrated that elongation of side chains of several sensitizers endowed them with higher affinity for artificial and natural membranes and caused their deeper localization in membranes. In the present study, we employed eight hematoporphyrin and protoporphyrin analogs and four groups containing three chlorin analogs each, all synthesized with variable numbers of methylenes in their alkyl carboxylic chains. We show that these tetrapyrroles' affinity for bovine serum albumin (BSA) and their localization in the binding site are also modulated by chain lengths. The binding constants of the hematoporphyrins and protoporphyrins to BSA increased as the number of methylenes was increased. The binding of the chlorins depended on the substitution at the meso position opposite to the chains. The quenching of the sensitizers' florescence by external iodide ions decreased as the side chains became longer, indicating to deeper insertion of the molecules into the BSA binding pocket. To corroborate this conclusion, we studied the efficiency of photodamage caused to tryptophan in BSA upon illumination of the bound sensitizers. The efficiency was found to depend on the side-chain lengths of the photosensitizer. We conclude that the protein site that hosts these sensitizers accommodates different analogs at positions that differ slightly from each other. These differences are manifested in the ease of access of iodide from the external aqueous phase, and in the proximity of the photosensitizers to the tryptophan. In the course of this study, we developed the kinetic equations that have to be employed when the sensitizer itself is being destroyed.

B. Ehrenberg ehren@mail.biu.ac.il.

Keywords

Albumin; Binding; Chlorin; Hematoporphyrin; Protoporphyrin; Photosensitization

Introduction

The interaction of photosensitizer molecules with proteins, artificial and natural membranes and cells has been a rich and active field of research in the recent 25 years, because of the advent of biological photosensitization and photo-dynamic therapy (PDT). PDT is a two-stage treatment of malignant tissues, which uses a photosensitizing drug and preferentially red, nonthermal, light. The photosensitizer absorbs light and generates cytotoxic singlet oxygen and other reactive oxygen species, leading to cellular damage (Henderson and Dougherty 1992; Pandey 2000; Smith and Hahn 2002; Verma et al. 2007). The strength of the PDT effect depends on the light dose that is absorbed, on the sensitizer concentration, on oxygen availability (Kreimer-Birnbaum 1989; Jori 1992) as well as on the photophysical parameters of the sensitizing compounds (Boyle and Dolphin 1996). Most of current research on PDT is focused on the treatment of cancer; however, other PDT applications should not be omitted, including autoimmune diseases, atherosclerosis and killing of microorganisms and viruses (Dougherty 2002; Jori and Brown 2004; Wainwright 2004).

Tetrapyrrole-based molecules, which are used as sensitizers, have a pronounced tendency to aggregate in aqueous solutions, and thus are mostly transported in blood and delivered to tumor cells either as aggregates or as proteinbound monomers. Dissociation or partial disaggregation of large aggregates occurs upon binding to serum proteins and within tumor cells. The type of protein-carrier conjugate governs the delivery of sensitizer to the tumor (Jori and Reddi 1993). Serum albumin, the most abundant protein in blood plasma, serves as a carrier for amphiphilic and hydrophilic photosensitizers (Kongshaug 1992); hydrophobic molecules bind preferentially to low-density lipoproteins and transferrin and are taken up by receptormediated endocytosis (Kongshaug et al. 1989). Carriers can be useful, especially when hydrophobic photosensitizers are employed (Dougherty et al. 1998; Rosenkranz et al. 2000). Conjugates of hematoporphyrin IX (HP3) with serum albumin and transferrin were prepared for application in biological photosensitization (Hamblin and Newman 1994).

In this work, we studied the effect of molecular structure of two groups of porphyrins and four groups of chlorins on their mode of binding to bovine serum albumin (BSA). We employed two series of hematoporphyrins and protoporphyrins, which were modified so that the alkyl carboxylate side chains of each molecule contained two, five or seven carbon atoms in each chain, in addition to natural hematoporphyrin IX (HP) and protoporphyrin IX (PP), which contain three carbon atoms in each chain. We also used four newly synthesized series of chlorins, which differ from each other by a major side group at the meso position and within each group they differ by the length of the alkyl carboxylate side chains, containing two, three or four carbon atoms. In previous studies (Lavi et al. 2001; Bronshtein et al. 2004; Bronshtein et al. 2005; Minnes et al. 2008; Ben Dror et al. 2009), we demonstrated that elongation of the side chains increased the affinity of the modified porphyrins for artificial membranes. It also caused a displacement of the bulk of the tetrapyrrole to a deeper location inside the lipid bilayer membrane. This, in turn, resulted in an increase in the observed efficiency of photosensitized degradation of membrane-residing singlet oxygen targets, because singlet oxygen had an opportunity to diffuse a longer distance in the membrane before escaping into the aqueous phase. It may also be the reason for an increased in situ photosensitization of cells that absorbed these sensitizers and even an increase in the in vivo PDT effect in mice (Bronshtein et al. 2006).

We report in this study that when the sensitizers were bound to BSA, iodide caused lesser quenching of their fluorescence as the sensitizer side chains increased in length, indicating that they were better shielded from an external iodide ion. We also show that singlet oxygen, which is generated by illumination of the sensitizers, causes differential damage to tryptophan in BSA. The present study thus demonstrates that modifications of side chains of the studied chlorins and porphyrins are manifested in the way these molecules are localized within the active site of albumin. The lipid:water interface of membranes is defined and it is thus not surprising that it can act as an anchoring point for amphiphilic photosensitizers. In the current manuscript we show, however, that delicate changes in the localization of the same chlorins, as well as porphyrins, can arise even in a case when these molecules are bound in the protein, with its less defined phase boundaries. These differences result in changes in the spectroscopic and photophysical properties of the bound sensitizers.

Materials and methods

Chemicals and sample preparation

Protoporphyrin IX and hematoporphyrin IX were obtained from Sigma (St. Louis, MO). The other protoporphyrin and hematoporphyrin derivatives, with alkyl carboxylate groups containing two, five or seven carbon atoms in each chain (Fig. 1), were custom synthesized for this project. These syntheses were accomplished from monopyrroles using the a,c-biladiene route (Holmes 1997). 2-Formyl-3,5-dimethylpyrroles bearing 4-ester side chains with different numbers of chain methylenes (n = 1,4,6) were individually reacted with the same dihydrodipyrrin to provide the corresponding a,c-biladiene salts; these were then cyclized using the copper(II) oxidation procedure (Smith 2000). All synthetic porphyrins were fully characterized using spectrophotometry, proton NMR spectroscopy and elemental analysis and/or high-resolution mass spectrometry. None showed evidence of any impurities. The proto- and hematoporphyrins are named HP2, PP2, HP3, PP3, HP5, PP5, HP7 and PP7, where the digit corresponds to the total number of carbon atoms in each of the two side chains.

The chlorins were synthesized using a new synthetic approach for chlorins (2 + 2 Method) (O'Neal et al.2006). This method is based on a variant of the MacDonald porphyrin synthesis (Arsenault et al. 1960) and involves condensation of bis-formyldihydrodipyrrins with symmetrical dihydrodipyrrins (Jacobi et al. 2001). By this approach the chlorin chromophore is obtained directly in the proper oxidation state and with no need for subsequent isomerization.

Stock solutions of the porphyrins (0.1 mM) and the chlorins (1 mM) were prepared in DMSO. Phosphatebuffered saline (PBS), at pH = 7.4, was used to prepare stock solutions of BSA (0.01 g/ml = 0.15 mM), KI (8 M) and $Na_2S_2O_3$ (0.2 M). KCl, up to a concentration of 0.15 M, in the case of the porphyrins and up to 0.24 M in the chlorins, was added to these buffer solutions in order to keep the total ionic strength constant.

Spectroscopic measurements

Absorption spectra were recorded on a Perkin-Elmer (Norwalk, CT) Lambda-9 UV–visible–near-IR, computer-controlled spectrophotometer and on a Shimadzu (Kyoto, Japan) UV-2501PC UV–vis spectrophotometer. Fluorescence excitation and emission spectra and fluorescence time-drive measurements were performed on a Perkin-Elmer LS-50B digital fluorimeter. For fluorescence measurements, all samples had optical density <0.05 at the wavelength of excitation, to maintain linear dependence of fluorescence intensity on concentration.

Measurement of binding constants to BSA

The sensitizers were added from their stock solutions in DMSO to PBS buffer, keeping the final volume of DMSO at <1% of the total volume of buffer. The final concentration of porphyrins in the samples was 0.1 μM. The binding constant, K_b, of each sensitizer to BSA was measured spectroscopically. K_b is defined as: $K_b = \frac{[P_{bound}]}{[P_{aqueous}] \cdot [M]}$, where $[P_i]$ is the concentration of the protein-bound, or aqueously dissolved porphyrin, and $[M]$ is the concentration of the binding protein. K_b is thus given in units of [protein concentration]$^{-1}$. After each addition of an aliquot of BSA from its stock, emission spectra were recorded following a very short incubation time of <1 min, at which equilibrium of binding was reached. For binding studies of HP derivatives we used λ_{ex} = 400 nm and λ_{em} = 623 nm. For binding of PP derivatives λ_{ex} = 402 nm and λ_{em} = 629 nm. For the chlorins binding, λ_{ex} = 400 nm and λ_{em} = 639–653 nm, according to each chlorin's emissions peak.

Fluorescence quenching by iodide ions

A set of samples was prepared for each porphyrin or chlorin derivative, containing the sensitizer (at 10^{-7} M), 10^{-5} M of $Na_2S_2O_3$ to prevent oxidation of I^- to colored I_2, and increasing concentrations of KI (0–0.15 M). All samples contained KCl, which was added to the KI to a total electrolyte concentration of 0.15 M, to maintain a constant ionic strength. The wavelengths at which the iodide quenching experiments were done were as outlined in the previous section. For these experiments, we used 0.015 g BSA/ml, a concentrations that is high enough to ensure that all the porphyrins were almost fully bound (>99%) to BSA. In the chlorins' measurements the sensitizer concentration was 1.5×10^{-7} M, KI concentrations increase to 0.24 M and the BSA concentration was 0.01 g/ml, which was high enough for all the chlorins to be fully bound (>99%) to BSA.

Damage to tryptophan in BSA by photosensitization

The tryptophan in BSA acts as a chemical trap of singlet oxygen, which is being generated upon illumination of the bound photosensitizers. Tryptophan's degradation in this process was monitored by following its fluorescence intensity. BSA concentration was 0.02 g/ml; the chlorin concentration was 3×10^{-6} M (this concentration is required to obtain a reliably measured absorbance). The intensity of tryptophan fluorescence was measured (λ_{ex} = 295 nm, λ_{em} = 340 nm) in a time-drive mode, while the sensitizer was being illuminated in situ in the fluorimeter by an Ar^+ laser (Stabilite 2017, Spectra-Physics, Mountain View, CA) beam at 501.7 nm. The illuminating laser beam passed along the cuvette's long axis, perpendicular to the fluorimeter excitation and emission directions. The laser power (around 30 mW) was measured at the sample surface with a power meter (model PD2-A, Ophir, Jerusalem, Israel), before and after the measurements, to ensure that the power remained constant during the experiment. The disappearance of tryptophan fluorescence followed decay kinetics, which will be detailed later.

Measurement of singlet oxygen quantum yields in methanol

The absolute quantum yields of production of singlet oxygen were measured by employing the singlet oxygen chemical trap 9,10 dimethylanthracene (DMA). The fluorescence of DMA disappears when it is oxidized by singlet oxygen and so the kinetics of the decrease of its fluorescence is measured for each studied sensitizer, in comparison to that generated by Rose Bengal, a standard sensitizer whose singlet oxygen yield is known. This method was described by us before (Sholto et al. 2008).

Results and discussion

Binding of derivatives of hematoporphyrin, protoporphyrin and chlorin to BSA

The uptake of various sensitizers by albumin, and other serum proteins, has been studied extensively in the literature (Reddi et al. 1987; Kongshaug 1992; Korbelik 1993; Gantchev et al. 1999). In this study, we were interested in evaluating the effect of structural modifications of the sensitizers on the affinities of their binding to BSA and on the location of the bound sensitizers. The following formula was used to evaluate the binding constant of the sensitizers to BSA, K_b (Ehrenberg 1992):

$$F = \frac{F_{init} + F_{comp} K_b [P]}{1 + K_b [P]} \quad (1)$$

F_{init} is the fluorescence intensity of the sensitizers, measured in the absence of protein; F is the intensity measured in the presence of protein at concentration [P]; F_{comp} is the fluorescence intensity, which is achieved asymptotically upon complete binding at infinite protein concentration. We measured the fluorescence intensity of the binding chromophores and the results of F versus [P] were fitted to the above function, to yield K_b and F_{comp}.

We did not observe aggregation of the studied sensitizers at the low concentrations (below 0.1 μM) that were used, as evident from the linear dependence of absorbance on concentration. Upon binding to proteins or to lipid membranes a remarkable increase in fluorescence intensities is observed (Aveline et al. 1995). The enhanced fluorescence intensity upon entering the lipid or protein domains is accompanied by the common red shift in the emission spectrum. With the HP derivatives the fluorescence peak shifts from 618 to 623 nm, in the case of PP derivatives the peak shifts from 620 to 629 nm, and with the chlorin derivatives the peak red-shifts by 3–10 nm, depending to the substituent at the meso position. The spectroscopic changes arise from different interactions of the chromophoric molecules with water and with the lipid or the protein cavity, as the polarity of the latter environments is lower than that of water. The binding constants of the studied sensitizers to BSA are presented in Table 1.

The binding constants of the four hematoporphyrins and four protoporphyrins to BSA exhibit a general increasing trend as the number of carbon atoms in the carboxylate chains increases. There is also a general trend that protoporphyrins bind better than hematoporphyrins with the same side chains. The trends are expected and are explainable on the basis of an increase in the hydrophobicity upon elongation of the alkyl carboxylate chains of the porphyrins, as was observed in many earlier cases (Kępczyński et al. 2002). The chlorins do not show a common behavior of binding to BSA. The groups with methyl and phenyl substituents (classes BX and CX, respectively) exhibit an increased binding to BSA as the length of the side chains increases. In contrast, group DX, with pentyl substitution exhibits a decreased BSA affinity as the chains lengthen. There is thus an inverse correlation between the lipophilicity of chlorins in this group and their affinity for BSA. Despite the accumulation of large amount of data regarding drug binding to plasma proteins, the prediction of this binding continues to be problematic (Kratochwil et al. 2002). In several cases, such as here, increased apolarity of a tetrapyrrole sensitizer is concomitant with lowered BSA binding while in many other instances the trend is reversed (Borissevitch et al. 1996; Bose and Dube 2006; Mishra et al. 2006). Group AX, without substitution at the meso position has a non-descript behavior.

To evaluate the numbers of albumin binding sites for the studied porphyrins and chlorins we resorted to another methodology. When the binding of a ligand to a protein site elicits static quenching to a fluorophore in the protein, such as tryptophan, the binding constant and the

number of binding sites can be calculated, using the following equation (Tian et al. 2003; Min et al. 2004):

$$\log\left(\frac{F_0 - F}{F}\right) = \log K_b + n \log [Q] \quad (2)$$

where F_0 and F are the fluorescence intensities of the tryptophan without and with the bound quencher (chlorin or porphyrin in our study), respectively, $[Q]$ is the concentration of this quencher, and K_b and n are the binding constant and number of binding sites, respectively. n can thus be obtained from the slope of a plot of $\log\left(\frac{F_0 - F}{F}\right)$ versus $\log[Q]$. K_b can, in principle, also be calculated, from the intersection of the fitted line with the y-axis. We found, however, that since the values of $[Q]$, namely the concentration of sensitizers, were in the range of 10^{-6}–7×10^{-6} M, the intercept was extremely sensitive to the calculated slope of the line. A small (<10%) change in this slope would have led to >70% variation in K_b. We used therefore Eq. 2 to calculate n only, and we preferred using Eq. 1 to calculate K_b. The values of n are shows in Table 1. As can be seen, in all the cases the result was very close to 1, indicating to one specific binding site of BSA for these tetrapyrrole sensitizers. A previous study also showed that BSA had one binding site for HP (Feng et al. 1996).

Fluorescence quenching of sensitizers bound to BSA

The quenching efficiency of fluorescing molecules by iodide ions was shown to be a tool in assessing the relative vertical depth of membrane-bound fluorophores, including porphyrins (Chalpin and Kleinfeld 1983; Cranney et al. 1983; Moro et al. 1993). We have demonstrated in previous studies, by employing fluorescence quenching methodologies, that the tetrapyrrole core of hematoporphyrins, protoporphyrins or dithiaporphyrins was located at larger depths in the membrane as the alkyl carboxylate side chain was made longer, containing from 2 up to 7 carbon atoms in a chain of the porphyrins and from 2 to 10 in the dithiaporphyrins (Lavi et al. 2001; Bronshtein et al. 2004; Minnes et al. 2008). We wanted to explore whether the exact location of sensitizers in albumin's binding site is also affected by similar modifications. We therefore employed here, too, fluorescence quenching by external iodide ions as an indicator for the sensitizer accessibility from the external aqueous phase. Fluorescence quenching is associated with a quenching constant, K_q, which is obtained from the Stern–Volmer Eq. 3:

$$\frac{F_0}{F} = 1 + K_q \tau_0 [Q] = 1 + K_q [Q] \quad (3)$$

F_0 and F are fluorescence intensities in the absence and in the presence of the quencher, respectively, whose concentration is $[Q]$. In order to obtain K_q for each studied derivative, data of F_0/F were plotted versus $[Q]$ and fitted to Eq. 3 by a linear regression routine.

Figure 2 shows, as an example, the quenching of chlorine AD by iodide. In all cases we obtained linear Stern–Volmer quenching plots, with y-axis intercepts very close to 1. We employed high enough BSA concentration, 0.01 g/ml, to ensure that practically all the sensitizers were bound to BSA and there were no different populations of fluorophores, in terms of their quenching ability. Iodide ions are known as dynamic, collisional, fluorescence quenchers and the linearity indicates that static quenching is not mixed with the collisional process. The population of the fluorescing sensitizer molecules inside the protein is accessible to iodide ions, which penetrate from the external aqueous solution and cause collisional dynamic quenching. The fact that the shape of the spectra did not change when iodide was added also indicates that the quenching process is collisional and there is no mechanism of static quenching.

If the effect of a sensitizer's depth in the BSA is to be deduced from the quenching of its fluorescence, the intrinsic, depth-independent, fluorescence quenching efficiency of each chromophore needs to be factored out. We achieve this by calculating the ratio between the fluorescence quenching constants in BSA and in buffer. When these ratios are compared, the influence of the fluorophore's localization and exposure to external iodide ions is singled out. We thus relate the quenching efficiencies that were observed in the non-isotropic restricted phase of BSA, to the quenching in a homogeneous phase, buffer ($K_{q,BSA}/K_{q,buf}$). By doing so, any intrinsic parameters that affect the quenching efficiency and are not related to the changed location in the BSA, are delineated. As Table 1 demonstrates, the net quenching efficiency of the BSA-bound sensitizers, which is due to the relative exposure of the sensitizers to the external water phase, decreases as the chains lengthen.

These quenching results thus indicate that the sensitizers' tetrapyrrole rings are located in the protein binding site at different distances from the external water phase. As the length of the side chains increases, the tetrapyrrole probably inserts and penetrates deeper into the BSA cavity and is thus less exposed to external quenching. It is possible that the charged carboxylates are anchored near the external, polar face of the globular protein.

Oxygenation of tryptophan photosensitized by bound sensitizers

We wished to corroborate the conclusion that was obtained from the iodide quenching experiments, that within a group of similar sensitizers, elongation of the side chains places the molecules at different positions in the albumin binding site. We thus measured the efficiency at which tryptophan is being degraded by photosensitization when the sensitizers were fully bound to the BSA. BSA has two tryptophan moieties, Trp135 and Trp212. The second one is located near the binding site of porphyrins (Silvester et al. 1998; Tian et al. 2007). The proximity of a bound tetrapyrrole sensitizer to tryptophan should result in faster photodegradation of the tryptophan by reaction with singlet oxygen, which is generated by the sensitizer. The effect on a further removed tryptophan is expected to be small. While attempting to carry out these experiments with the chlorins, we noticed that they underwent self-photodestruction. The rate of this deterioration was not negligible compared to the rate at which the tryptophan was photodamaged. The situation of a photosensitization reaction in which the sensitizer itself is being photodamaged is quite common in photochemistry and photobiology (Rotomskiene et al. 1988; Rotomskis et al. 1996). This is also manifested strongly when photosensitizers in cells are observed under fluorescence microscopy. There is indication that self-photobleaching of some porphyrins and chlorin e6 was enhanced when these molecules were bound to human serum albumin (Bagdonas and Jasaitis 1997). Evaluation of the sensitization of a target can still be obtained in such situation, with the aid of the following kinetics that we have developed.

The intensity of light that is absorbed by the sensitizer, I_{abs}, in a sample whose optical density at the illuminating wavelength is OD, is given by Eq. 4:

$$I_{asb}=I_0 \cdot \left(1 - 10^{-OD}\right) \quad (4)$$

I_0 is the intensity of incident light. If the initial optical density of the sensitizer, OD_0, is small, the following linearized series expansion can be taken:

$$I_{asb}=I_0 \cdot 2.3 \cdot OD \quad (5)$$

The rate at which light is being absorbed by the sensitizer, whose concentration diminishes exponentially with a rate of k_s, due to self-destruction, is:

$$k_{asb}=A \cdot 2.3 \cdot OD_0 \cdot e^{-k_s t} \quad (6)$$

where A contains the power of the laser. The destruction of a chemical target, T, by singlet oxygen that is generated by photosensitization is given by:

$$\frac{dT}{dt}=-\varphi_\Delta \cdot A \cdot 2.3 \cdot OD_0 \cdot e^{-k_s t} \cdot T \quad (7)$$

ϕ_Δ is the singlet oxygen production yield. The solution of this differential equation is:

$$\ln T=\ln T_0+\frac{\varphi_\Delta \cdot 2.3 \cdot OD_0}{k_s}\left(e^{-k_s t}-1\right) \quad (8)$$

If the sensitizer is stable, namely if k_s approaches 0, the right term in Eq. 8 has both a numerator and denominator that approach zero. According to l'Hospital's rule:

$$\lim_{k_s \to 0}\left(\frac{e^{-k_s t}-1}{k_s}\right)=\lim_{k_s \to 0}\frac{\left(e^{-k_s t}-1\right)'}{(k_s)'}=-t \quad (9)$$

Under this condition, Eq. 8 evolves into the usual formula: $T=T_0 e^{-(2.3 \cdot \phi_\Delta \cdot OD \cdot A) \cdot t}$. Thus, when the sensitizer itself is being destroyed, one should monitor the disappearance of the chemical target, usually spectroscopically, and fit the data to Eq. 2Eq. 8 to extract ϕ_Δ. Figure 3 shows an example for fitting Eq. 8 to the degradation of BSA's tryptophan by photosensitization of the chlorin DB, which undergoes self-destruction under light. As can be seen, the logarithm of tryptophan's fluorescence intensity is not a linear function of time but indeed exponential.

Table 1 shows results of the sensitization of tryptophan by the different protoporphyrins, hematoporphyrins and chlorins. Here, too, we wanted to separate the effect of the sensitizer's proximity to a near tryptophan from the intrinsic singlet oxygen production yield by the sensitizer. We did this even though the differences in the net singlet oxygen production efficiency between sensitizers within each group are very small, between 5 and 8%. Thus the relative values of the quantum yields of photo-degradation of tryptophan were divided by the intrinsic singlet oxygen production yields of the sensitizers in a homogeneous solution, without BSA. The values in the Table are normalized relative to the photodestruction efficiency that is caused by PP3, HP5 and chlorin CD, respectively, which were the most efficient destroyers of tryptophan among each group. These results indicate that the efficiency at which tryptophan is being damaged depends on the nature of the sensitizer, even after the small differences in the intrinsic singlet oxygen yields were accounted for. One can infer from these results that for the hematoporphyrins and the chlorins with phenyl substitution at the meso position, CX, elongation of the alkyl carboxylate chains brings them to be located closer to the tryptophan in BSA, and the normalized ϕ_D increases. In contrast, the three chlorins without substitution at the fifth position, AX, are bound to BSA in such a way that places the analog with the short chain, AB, closer to the nearest tryptophan than those with longer chains, AC and AD. A similar trend is seen for the chlorins bearing a pentyl group, DB, DC and DD. For the protoporphyrins and the chlorins with methyl substitution, the analog with a medium chain length, PP3 and BC, respectively, are placed optimally relative to the tryptophan. As control experiments we monitored tryptophan's degradation in identical samples which were bubbled with nitrogen, and contained 0.1 M sodium azide, a known physical quencher of singlet oxygen. In such circumstances no decrease in BSA's tryptophan fluorescence was

observed upon illumination of the bound sensitizer. This proves that the damage that is inflicted to tryptophan is indeed caused by photogenerated singlet oxygen.

One could also consider the option that the differences between the tryptophan damage kinetics arise not only from the proximity of the bound sensitizer to the tryptophan, but also from variations in the singlet oxygen yield by the bound sensitizers due to the effect of their location in the albumin. These intrinsic differences in the ϕ_{Δ}, which might arise from the exact location of the sensitizer in the binding site could not be factored out, for the following reason. We found that when the albumin-bound sensitizers are illuminated in the presence of a water-solubilized chemical target of singlet oxygen, 9,10-anthracene dipropionic acid, no significant destruction of this target could be observed. However, the same target was destroyed very rapidly when both it and the sensitizers were in water, without BSA. We conclude that singlet oxygen, which is generated by BSA-bound sensitizers, is scavenged very efficiently by the tryptophan in BSA, which is close to it, as well as by other aromatic acids and also by physical quenching by the protein in which it was generated. However, even if differences in the location of the sensitizers in the albumin had an effect on singlet oxygen's yield, as mentioned above, it corroborates our claim that changes in the side chains of the sensitizers cause their placement at different positions in the protein's binding site. In this context, we measured the fluorescence quantum yields (ϕ_F) of the chlorin sensitizers in methanol as well as when bound to BSA, in comparison to rhodamine 101 as a fluorescent standard, and found them to have very small variations. We thus think that the intrinsic yield of singlet oxygen is also not varying and the differences in the photodestruction of tryptophan are mainly a proximity effect.

The trends of the data of fluorescence quenching by iodide and tryptophan photodamaging cannot be mapped to each other, because they reflect non-correlated attributes. The first depends on the accessibility of the bound chromophore to iodide ions that come from the external aqueous medium while the latter reflects the proximity of the chromophore to tryptophan within the BSA structure. The results do corroborate, however, the notion that slight elongation of the side-chain affects the exact position of the sensitizers within BSA and this is reflected in both measured parameters.

Conclusion

We showed in this study that the strength and mode of binding of derivatized hematoporphyrins, protoporphyrins and chlorins to BSA depends, for each of these groups, on the chemical structures of the molecule. Most importantly, we show that the position of the sensitizers within the protein binding site is affected by the length of the alkyl carboxylate side chains, which were incrementally modified in all the studied groups of molecules.

Acknowledgments

We thank Mr. Hui Wang, who prepared several of the chlorin samples. We acknowledge the support (Grant No. 2002-383) of the United States-Israel Binational Science Foundation (BSF), Jerusalem, Israel (to K. M. S. and B. E.) We also acknowledge the support of the Michael David Falk Chair in Laser Phototherapy (to B. E.). Financial support of this work by the National Institutes of Health, NIGMS Grant No. GM38913 (to P. A. J.) is gratefully acknowledged.

Abbreviations

BSA	Bovine serum albumin
DMA	9,10 Dimethylanthracene

HP3	Hematoporphyrin IX
PBS	Phosphate-buffered saline
PDT	Photodynamic therapy
PP3	Protoporphyrin IX
DMSO	Dimethyl sulfoxide

References

Arsenault GP, Bullock E, MacDonald SF. Pyrromethanes and porphyrins therefrom. J Am Chem Soc. 1960; 82:4384–4395. doi:10.1021/ja01501a066.

Aveline BM, Hasan T, Redmond RW. The effects of aggregation, protein binding and cellular incorporation on the photophysical properties of benzoporphyrin derivative monoacid ring A (BPDMA). J Photochem Photobiol B Biol. 1995; 30:161–169.

Bagdonas S, Jasaitis A. Photostability of sensitizers in various model systems: a spectroscopic study. Biologija (Vilnius). 1997; 1:81–86.

Ben Dror S, Bronshtein I, Garini Y, O'Neal WG, Jacobi PA, Ehrenberg B. The localization and photosensitization of modified chlorin photosensitizers in artificial membranes. Photochem Photobiol Sci. 2009 (in press). doi:10.1039/B814970D.

Borissevitch IE, Tominaga TT, Imasato H, Tabak M. Fluorescence and optical absorption study of interaction of two water soluble porphyrins with bovine serum albumin. The role of albumin and porphyrin aggregation. J Lumin. 1996; 69:65–76. doi:10.1016/0022-2313(96)00037-3.

Bose B, Dube A. Interaction of chlorin p6 with bovine serum albumin and photodynamic oxidation of protein. J Photochem Photobiol B Biol. 2006; 85:49–55.

Boyle RW, Dolphin D. Structure and biodistribution relationships of photodynamic sensitizers. Photochem Photobiol. 1996; 64:469–485. doi:10.1111/j.1751-1097.1996.tb03093.x. [PubMed: 8806226]

Bronshtein I, Afri M, Weitman H, Frimer AA, Smith KM, Ehrenberg B. Porphyrin depth in lipid bilayers as determined by iodide and parallax fluorescence quenching methods and its effect on photosensitizing efficiency. Biophys J. 2004; 87:1155–1164. doi:10.1529/biophysj.104.041434. [PubMed: 15298918]

Bronshtein I, Smith KM, Ehrenberg B. The effect of pH on the topography of porphyrins in lipid membranes. Photochem Photobiol. 2005; 81:446–451. doi:10.1562/2004-09-12-RA-316.1. [PubMed: 15581389]

Bronshtein I, Aulova S, Juzeniene A, Iani V, Ma LW, Smith KM, Malik Z, Moan J, Ehrenberg B. In vivo and in vitro photosensitization by protoporphyrins possessing different lipophilicities and vertical localization in the membrane. Photochem Photobiol. 2006; 82:1319–1325. doi: 10.1562/2006-04-02-RA-865. [PubMed: 16740058]

Chalpin DB, Kleinfeld AM. Interaction of fluorescent quenchers with the n-(9-anthroyloxy) fatty acid membrane probes. Biochim Biophys Acta. 1983; 731:465–474. doi: 10.1016/0005-2736(83)90042-1.

Cranney M, Cundall RB, Jones GR, Richards JT, Thomas EW. Fluorescence lifetime and quenching studies on some interesting diphenylhexatriene membrane probes. Biochim Biophys Acta. 1983; 735:418–425. doi:10.1016/0005-2736(83)90156-6.

Dougherty TJ. An update on photodynamic therapy applications. J Clin Laser Med Surg. 2002; 20:3–7. doi:10.1089/104454702753474931. [PubMed: 11902352]

Dougherty TJ, Gomer CJ, Henderson BW, Jori G, Kessel D, Korbelik M, Moan J, Peng Q. Photodynamic therapy. J Natl Cancer Inst. 1998; 90:889–905. doi:10.1093/jnci/90.12.889. [PubMed: 9637138]

Ehrenberg B. Assessment of the partitioning of probes to membranes by spectroscopic titration. J Photochem Photobiol B Biol. 1992; 14:383–386. doi:10.1016/1011-1344(92)85117-D.

Feng XZ, Jin RX, Qu Y, He XW. Studies of the ions' effect on the binding constant between HP and BSA. Chem J Chin Univ. 1996; 17:866–869.

Gantchev TG, Ouellet R, Vanlier JE. Binding interactions and conformational changesinduced by sulfonated aluminum phthalocyanines in human serum albumin. Arch Biochem Biophys. 1999; 366:21–30. doi:10.1006/abbi.1999.1174. [PubMed: 10334859]

Hamblin MR, Newman EL. Photosensitizer targeting in photodynamic therapy. I. Conjugates of haematoporphyrin with albumin and transferrin. J Photochem Photobiol B Biol. 1994; 26:45–56. doi:10.1016/1011-1344(94)85035-6.

Henderson BW, Dougherty TJ. How does photodynamic therapy work? Photochem Photobiol. 1992; 55:145–157. doi:10.1111/j.1751-1097.1992.tb04222.x. [PubMed: 1603846]

Holmes, RT. Ph.D. thesis. University of California; Davis: 1997. Synthetic Studies of Poly-Pyrrolic Macrocycles.

Jacobi PA, Lanz S, Ghosh I, Leung SH, Lower F, Pippin D. A new synthesis of chlorins. Org Lett. 2001; 3:831–834. doi:10.1021/ol006983m. [PubMed: 11263893]

Jori G. Far-red absorbing photosensitizers: their use in the photodynamic therapy of tumours. J Photochem Photobiol A. 1992; 62:371–378. doi:10.1016/1010-6030(92)85065-3.

Jori G, Brown SB. Photosensitized inactivation of microorganisms. Photochem Photobiol Sci. 2004; 3:403–405. doi:10.1039/b311904c. [PubMed: 15122355]

Jori G, Reddi E. The role of lipoproteins in the delivery of tumour-targeting photosensitizers. Int J Biochem. 1993; 25:1369–1375. doi:10.1016/0020-711X(93)90684-7. [PubMed: 8224351]

Kępczyński M, Pandian RP, Smith KM, Ehrenberg B. Do liposome-binding constants of porphyrins correlate with their measured and predicted partitioning between octanol and water? Photochem Photobiol. 2002; 76:127–134. doi:10.1562/0031-8655(2002)076<0127:DLBCOP>2.0.CO;2. [PubMed: 12194207]

Kongshaug M. Distribution of tetrapyrrole photosensitizers among human plasma proteins. Int J Biochem. 1992; 24:1239–1265. doi:10.1016/0020-711X(92)90200-K. [PubMed: 1644211]

Kongshaug M, Moan J, Brown SB. The distribution of porphyrins with different tumor localizing ability among human plasma proteins. Br J Cancer. 1989; 59:184–188. [PubMed: 2930683]

Korbelik M. Cellular delivery and retention of photofrin: III. Role of plasma proteins in photosensitizer clearance from cells. Photochem Photobiol. 1993; 57:846–850. doi:10.1111/j.1751-1097.1993.tb09222.x. [PubMed: 8337259]

Kratochwil NA, Huber W, Muller F, Kansy M, Gerber PR. Predicting plasma protein binding of drugs: a new approach. Biochem Pharmacol. 2002; 64:1355–1374. doi:10.1016/S0006-2952(02)01074-2. [PubMed: 12392818]

Kreimer-Birnbaum M. Modified porphyrins, chlorins, phthalocyanines, and purpurins: second generation photosensitizers for photodynamic therapy. Semin Hematol. 1989; 26:157–173. [PubMed: 2658091]

Lavi A, Weitman H, Holmes RT, Smith KM, Ehrenberg B. The depth of porphyrin in a membrane and the membrane's physical properties affect the photosensitizing efficiency. Biophys J. 2001; 82:2101–2110. doi:10.1016/S0006-3495(02)75557-4. [PubMed: 11916866]

Min J, Meng-Xia X, Dong Z, Yuan L, Xiao-Yu L, Xing C. Spectroscopic studies on the interaction of cinnamic acid and its hydroxyl derivatives with human serum albumin. J Mol Struct. 2004; 692:71–80. doi:10.1016/j.molstruc.2004.01.003.

Minnes R, Weitman H, Youngjae Y, Detty MR, Ehrenberg B. Dithiaporphyrin derivativesas photosensitizers in membranes and cells. J Phys Chem B. 2008; 112:3268–3276. doi:10.1021/jp0768423. [PubMed: 18278897]

Mishra PP, Patel S, Datta A. Effect of increased hydrophobicity on the binding of two model amphiphilic chlorin drugs for photodynamic therapy with blood plasma and its components. J Phys Chem B. 2006; 110:21238–21244. doi:10.1021/jp0615858. [PubMed: 17048951]

Moro F, Goni FM, Urbaneja MA. Fluorescence quenching at interfaces and the permeation of acrylamide and iodide across phospholipid bilayers. FEBS Lett. 1993; 330:129–132. doi:10.1016/0014-5793(93)80257-U. [PubMed: 8365482]

O'Neal WG, Roberts WP, Ghosh I, Wang H, Jacobi PA. Studies in chlorin chemistry. 3. A practical synthesis of C, D-ring symmetric chlorins of potential utility in photodynamic therapy. J Org Chem. 2006; 71:3472–3480. doi:10.1021/jo060041z. [PubMed: 16626128]

Pandey RK. Recent advances in photodynamic therapy. J Porphyr Phthal. 2000; 4:368–373. doi: 10.1002/(SICI)1099-1409(200006/07)4:4<368::AID-JPP244>3.0.CO;2-6.

Reddi E, Lambert CR, Jori G, Rodgers MAJ. Photokinetic and photophysical measurements of the sensitized photo oxidation of the tryptophyl residue in NATA and in human serum albumin. Photochem Photobiol. 1987; 45:345–351. doi:10.1111/j.1751-1097.1987.tb05385.x. [PubMed: 3562591]

Rosenkranz AA, Jans DA, Sobolev AS. Targeted intracellular delivery of photosensitizers to enhance photodynamic efficiency. Immunol Cell Biol. 2000; 78:452–464. doi:10.1046/j.1440-1711.2000.00925.x. [PubMed: 10947873]

Rotomskiene J, Kapociute R, Rotomskis R, Jonusauskas G, Szito T, Nizhnik A. Light-induced transformations of hematoporphyrin diacetate and hematoporphyrin. J Photochem Photobiol B Biol. 1988; 2:373–379. doi:10.1016/1011-1344(88)85056-5.

Rotomskis R, Bagdonas S, Streckyte G. Spectroscopic studies of photobleaching and photoproduct formation of porphyrins used in tumour therapy. J Photochem Photobiol B Biol. 1996; 33:61–67. doi:10.1016/1011-1344(95)07228-4.

Sholto A, Lee S, Hoffman BM, Barrett AGM, Ehrenberg B. Spectroscopy, binding to liposomes and production of singlet oxygen by porphyrazines with modularly variable water solubility. Photochem Photobiol. 2008; 84:764–773. doi:10.1111/j.1751-1097.2007.00268.x. [PubMed: 18208451]

Silvester JA, Timmins GS, Davies MJ. Photodynamically generated bovine serum albumin radicals: evidence for damage transfer and oxidation at cysteine and tryptophan residues. Free Radic Biol Med. 1998; 24:754–766. doi:10.1016/S0891-5849(97)00327-4. [PubMed: 9586806]

Smith, KM. Strategies for the syntheses of octaalkylporphyrin systems. In: Kadishb, KM.; Smith, KM.; Guilard, R., editors. The porphyrin handbook. Vol. vol 1. Academic Press; Boston: 2000. p. 25-28.chap 1

Smith RP, Hahn SM. Photodynamic therapy. Curr Probl Cancer. 2002; 26:67–108. doi:10.1067/mcn.2002.125408. [PubMed: 12042761]

Tian JN, Liu JQ, Zhang JY, Hu Z, Chen X. Fluorescence studies on the interactions of barbaloin with bovine serum albumin. Chem Pharm Bull. 2003; 51:579–582. doi:10.1248/cpb.51.579. [PubMed: 12736459]

Tian JN, Liu X, Zhao Y, Zhao S. Studies on the interaction between tetraphenylporphyrin compounds and bovine serum albumin. Luminescence. 2007; 22:446–454. doi:10.1002/bio.983. [PubMed: 17610308]

Verma S, Watt GM, Mal Z, Hasan T. Strategies for enhanced photodynamic therapy effects. Photochem Photobiol. 2007; 83:996–1005. doi:10.1111/j.1751-1097.2007.00166.x. [PubMed: 17880492]

Wainwright M. Photoinactivation of viruses. Photochem Photobiol Sci. 2004; 3:406–411. doi:10.1039/b311903n. [PubMed: 15122356]

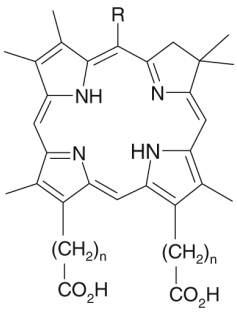

chlorins

n	R	compound
2	H	AB
3		AC
4		AD
2	Me	BB
3		BC
4		BD
2	Ph	CB
3		CC
4		CD
2	C_5H_{11}	DB
3		DC
4		DD

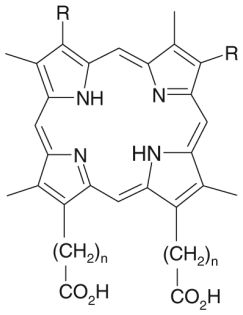

Protoporphyrins (PP)

R = -CH=CH_2

Hematoporphyrins (HP)

R = -CH(OH)-CH_3

n=1,2,4,6

Fig. 1.

Chemical structures of HP, PP and chlorins and their modified analogs

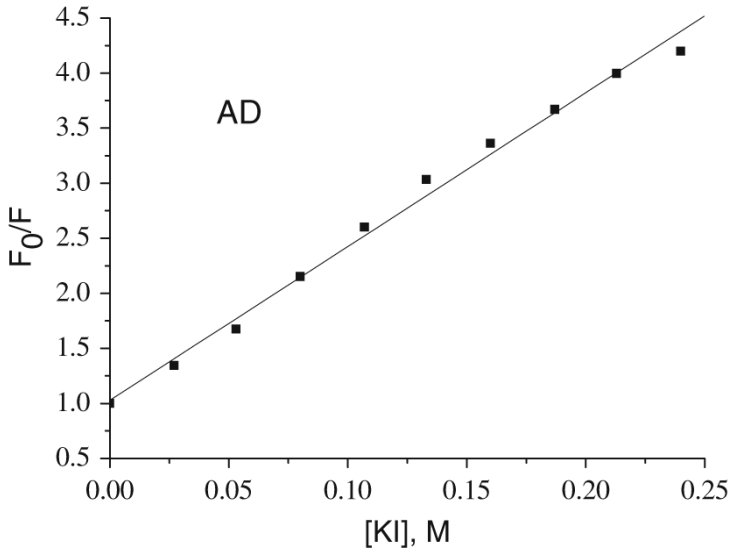

Fig. 2.
Stern–Volmer quenching plots for compound AD (150 nM) in PBS, pH = 7.20. Fluorescence intensities were excited at 400 nm and measured at 645 nm

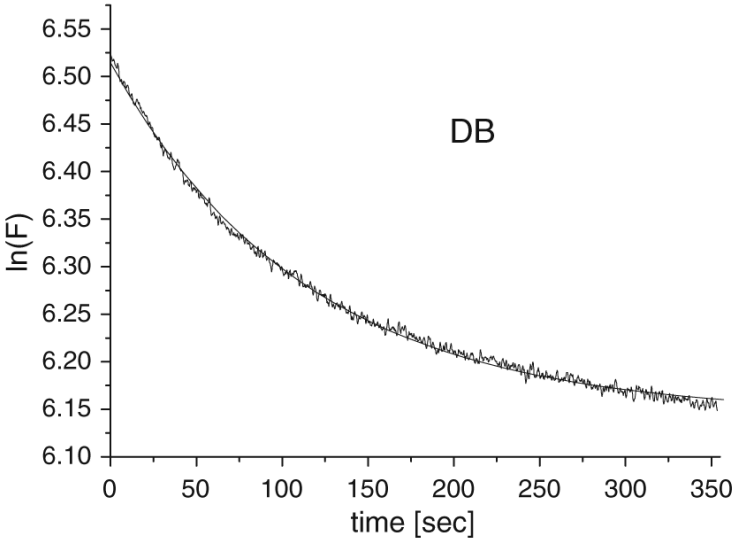

Fig. 3.

Photodamaging of tryptophan (λ_{ex} = 295 nm, λ_{em} = 340 nm) in BSA (20 mg/ml) by the chlorin analog DB (3 μM). The logarithm of tryptophan's fluorescence intensity is plotted versus time and fitted to Eq. 8

Table 1

(1) Binding constants, K_b, of the sensitizers (0.1 μM) to BSA. (2) Numbers of binding sites in BSA, *n*. (3) Γ fluorescence quenching constants of the sensitizers when bound to BSA relative to the quenching when dissolved in buffer. [BSA] = 15 mg/ml for HP and PP and 10 mg/ml for chlorins. [PP] = [HP] = 0.33 μM; [chlorins] = 0.15 μM. (4) Comparative efficiencies of singlet oxygentriggered photooxidation of BSA tryptophan, ϕ. The data in each group are normalized to the sensitizer that had the highest relative efficiency

Sensitizer	K_b to BSA $(mg/ml)^{-1}$	*n*	K_{BSA}/K_{PBS}	Normalized ϕ_Δ
HP2	13.63	1.0[a]	0.86	0.36 ± 0.03
HP3	10.13 ± 0.50	1.0[a]	0.76	0.79 ± 0.06
HP5	36.10 ± 4.86	1.0[a]	0.48	1.00 ± 0.09
HP7	82.91 ± 13.75	1.0[a]	0.38	0.96 ± 0.10
PP2	17.94 ± 5.12	0.989 ± 0.087	2.71	0.43 ± 0.04
PP3	21.61 ± 4.26	0.993 ± 0.082	1.38	1.00 ± 0.10
PP5	45.27 ± 6.27	0.998 ± 0.028	1.06	0.75 ± 0.10
PP7	111.05 ± 18.06	0.989 ± 0.097	0.65	0.38 ± 0.04
AB	46.84 ± 12.08	1.059 ± 0.028	0.28	0.25 ± 0.03
AC	103.61 ± 27.73	1.205 ± 0.039	0.18	0.13 ± 0.01
AD	45.43 ± 15.05	0.945 ± 0.040	0.15	0.11 ± 0.01
BB	41.27 ± 8.94	0.934 ± 0.112	0.40	0.41 ± 0.07
BC	103.55 ± 21.76	0.885 ± 0.065	0.34	0.51 ± 0.08
BD	124.54 ± 19.78	0.996 ± 0.039	0.18	0.41 ± 0.07
CB	162.82 ± 9.80	0.966 ± 0.027	0.52	0.33 ± 0.05
CC	171.69 ± 23.48	1.032 ± 0.009	0.33	0.59 ± 0.11
CD	232.53 ± 17.58	0.954 ± 0.019	0.15	1.00 ± 0.25
DB	204.06 ± 20.62	1.231 ± 0.091	0.60	0.78 ± 0.08
DC	81.74 ± 11.44	0.727 ± 0.158	0.19	0.27 ± 0.05
DD	72.05 ± 9.11	1.095 ± 0.005	0.06	0.31 ± 0.03

[a]Min et al. 2004